Fall 2007

# Microfluidic biosensors for intelligent metabolite monitoring

Nitin Radhakrishnan



Department:

# MICROFLUIDIC BIOSENSORS FOR INTELLIGENT METABOLITE MONITORING

by

NITIN RADHAKRISHNAN

A THESIS

Presented to the Faculty of the Graduate School of the

UNIVERSITY OF MISSOURI-ROLLA

In Partial Fulfillment of the Requirements for the Degree

MASTER OF SCIENCE IN ELECTRICAL ENGINEERING

2007

Approved by

| | |
|---|---|
| _____ | _____ |
| Chang-Soo Kim, Advisor | Minsu Choi |

_____

David Henthorn

## PUBLICATION THESIS OPTION

This thesis has been prepared in the form of two manuscripts for publication. An Introduction section has been included in the thesis to provide background information.

The first manuscript (pages 5-22) has been presented as a conference proceeding in the SPIE Optics East conference held at Boston, MA, USA on September 11th, 2007.

The second manuscript (pages 23-44) is intended for submission to BIOSENSORS AND BIOELECTRONICS JOURNAL.

## ABSTRACT

Baseline (zero-value) drift and sensitivity degradation are two common problems related with biosensors. In order to overcome these problems, there is a great need for integrating an on-demand, *in situ* self-diagnosis and self-calibration unit along with the sensor. Utilizing the microfluidic technology, it is possible to explore the feasibility of implementing this function without any externally coupled bulky apparatus. A microsystem including a microfluidic channel and calibration electrodes are prepared by microfabrication techniques. A novel method of using hydrogen and oxygen bubbles generated by electrolysis of water is used to saturate the solution with these gases in the microfluidic channel where the biosensor is placed. The hydrogen bubble provides oxygen-depleted microenvironment to conduct a zero-value calibration procedure for the sensor. The oxygen bubble provides high sensitivity and constant oxygen background environment to allow stable enzyme reactions that is not limited or perturbed by the fluctuation of background oxygen in sample solutions. Commercial oxygen and pH sensors are used to confirm whether saturation or depletion of oxygen has occurred with minimum local pH change near the sensor during the electrolytic bubble generation. Chronoamperometric tests are run on both glucose and creatinine sensors. Enhancement in signal-to-noise (S/N) ratio during oxygen amplification in the presence of interferents is also verified. The glucose and creatinine data obtained from the experiments assure that the proposed method is promising to overcome the above mentioned two problems.

# ACKNOWLEDGMENTS

I would like to express my utmost gratitude and thankfulness to my advisor Dr. Chang-Soo Kim for his constant support and guidance throughout the course of my Master's degree.

I wish to extend a special thank to my committee members, Dr. David Henthorn and Dr. Minsu Choi for their valuable input towards my work.

I wish to thank my lab partners, Jongwon Park and Raghu Ambekar Rao, for their assistance and moral support.

Finally, I thank my parents and sister for their emotional support and encouragement which they have been constantly providing me. I wish to dedicate this work to them.

# TABLE OF CONTENTS

Page

# LIST OF ILLUSTRATIONS

# 1. INTRODUCTION

## 1.1 BIOSENSORS AND THEIR PROBLEMS

Biosensors come under a special class of transducers that utilize some biological or living material for their sensing operation [1]. Transducers help to convert some form of signal to an electrical signal. In a typical biosensing application there is usually an analyte, biological material, and sensor [2]. The analyte is the biological quantity that needs to be measured which includes a wide variety that includes glucose, creatinine, lactate, sucrose, etc. Next in line is the biological material. The biological material acts as an intermediate between the analyte and the sensor. It can be enzymes, amino acids, or antibodies. They interact with the input analyte and give the output to the sensor. The sensor is usually realized using an electrochemical arrangement in the form of a cell that has an anode and cathode. In glucose and creatinine amperometric sensors, hydrogen peroxide ($H_2O_2$) is the final product formed by the biological sensing material. This is converted to an electrical signal by applying an appropriate bias voltage between the electrodes of the cell. The two most common problems with biosensors are baseline (zero-value) drift and sensitivity degradation. In order to circumvent these problems, there is a great need for integrating an on-demand, *in situ*, self-diagnosis and self-calibration unit along with the sensor. By performing electrolysis of water, it is possible to generate either a hydrogen bubble or oxygen bubble to manipulate the oxygen microenvironment around the enzyme (oxidase) based sensor. The hydrogen bubble provides oxygen-depleted microenvironment to conduct a one-point (zero-value) calibration procedure for the sensor since the oxidase reaction cannot be completed

without oxygen. On the other hand, the oxygen bubble helps in increasing the dynamic range and sensitivity of the sensor by providing constant oxygen-saturated environment. In the previous method of one-point, *in situ*, self-calibration [3], the hydrogen and oxygen bubbles were shifted below the biosensor placed in a microfluidic channel in such a way that the biosensor tip was completely surrounded by the respective bubble. Tests based on this procedure sometimes showed inconsistent and erroneous results. It was considered that the bubbles were drying up the enzyme layer located at the biosensor tip during the calibration phase. Another possible reason is that the reaction byproducts accumulate within the enzyme layer since it is disconnected from the bulk solution by the surrounding bubble. This required an improvement to the present calibration technique. The new method of calibration involves generating hydrogen or oxygen bubbles relatively close to the sensor and shifting the respective bubble short distances towards the sensor. When a hydrogen bubble is generated and shifted towards the location of the biosensor, the oxygen-depleted environment prevents the enzyme reaction to take place. This mimics an analyte-free environment even in the presence of the analyte in sample solutions and provides the environment for zero-value calibration. On the other hand, when an oxygen bubble is generated and shifted, the environment near the sensor is saturated with oxygen for enzyme reaction and is thus not limited by the oxygen availability in the solution. This helps in sensitivity enhancement because the enzyme reaction is not limited by oxygen. The increased sensitivity due to the oxygen bubbles effectively suppresses the noise ratio caused by electrochemical interferents.

## 1.2 TYPES OF SENSORS USED

In the two publication proceedings, glucose sensors and creatinine sensors have been used. The sensors are similar in their sensing mechanism and differ only in the enzymes used as the biological sensing material.

**1.2.1 Glucose Sensors.** In glucose (ß-D-Glucose) sensors, the analyte that needs to be measured is glucose. Glucose oxidase (GOD) is the enzyme that is used as the biological sensing material. Glucose detection is based on the amperometric detection of hydrogen peroxide caused by the oxidation of glucose catalyzed in the presence of glucose oxidase (GOD) enzyme [3], [4], [5]. The reaction is as follows:

$$\text{ß-D-Glucose} + O_2 \xrightarrow{\text{GOD}} \text{Gluconic acid} + H_2O_2$$

The working electrode of glucose sensor is biased positive (0.8V) with respect to the reference electrode for the detection of hydrogen peroxide. The measurements can be realized using the new calibration technique.

**1.2.2 Creatinine Sensors.** In creatinine sensors, the analyte that is measured is creatinine. Three enzymes are used for the detection mechanism. They are creatinine amidohydrolase (CA), creatine amidinohydrolase (CI) and sarcosine oxidase (SO). These enzymes help to sequentially convert creatinine to creatine and finally, to sarcosine and hydrogen peroxide [6], [7], [8], [9], [10], [11], [12]. The reactions in the tri-enzyme matrix are as given below:

$$\text{Creatinine} + H_2O \xrightarrow{\text{CA}} \text{Creatine}$$

$$\text{Creatine} + H_2O \xrightarrow{\text{CI}} \text{Sarcosine} + \text{Urea}$$

$$\text{Sarcosine} + H_2O + O_2 \xrightarrow{\text{SO}} \text{Glycine} + \text{Formaldehyde} + H_2O_2$$

The sensor measures $H_2O_2$ amperometrically same as like that of glucose sensor.

## REFERENCES

[1] M. Lambrechts and W. Sansen, Biosensors: microelectrochemical devices, Institute of Physics Publishing, 1992.

[2] G.T.A. Kovacs, Micromachined transducers sourcebook, 1998.

[3] Park, J., Kim, C.S., Choi, M., IEEE Transactions on Instrumentation and Measurement, Vol. 55, No. 4, pp. 1348-1355, August 2006.

[4] Kim, C.S., Lee, C.H., Fiering, J.O., Ufer, S., Scarantino, C.W., Nagle, H.T., IEEE Sensors Journal, Vol.4, No.5, pp. 568-575, October 2004.

[5] Park, J., Kim, C.S., Kim, Y., Sensors and Actuators B, Chem., Vol.108, No.1-2, pp. 633-638, 2005.

[6] Tsuchida, T., Yoda, K., Clinical Chemistry, Vol. 29, No. 1, pp. 55-55, 1983.

[7] Madaras, M.B., Buck, R.P., Analytical Chemistry, Vol. 68, No.21, November 1996.

[8] Erlenkotter, A., Fobker, M., Chemnitius, G.C., Analytical and Bioanalytical Chemistry, Vol. 372, No.2, pp. 284-292, 2002.

[9] Nguyen, V.K., Wolff, C.M., Seris, J.L., Schwing, J.P., Analytical Chemistry, Vol. 63, No. 6, pp. 611-614, 1991.

[10]Madaras, M.B., Popescy, I.C., Ufer, S., Buck, R.P., Analytica Chimica Acta, Vol. 319, No.3, pp.335-345, 1996.

[11]Yamato, H., Ohwa, M., Wernet, W., Analytical Chemistry, Vol. 67, pp. 2776-2780, 1996.

[12]Khan, G. F., Wernet, W., Analytica Chimica Acta, Vol. 351, No.1, pp. 151-158, 1997.

# Microfluidic biosensors for intelligent metabolite monitoring

Nitin Radhakrishnan[1], Jongwon Park[1], Chang-Soo Kim[1, 2]

[1] *Department of Electrical & Computer Engineering, UMR, Rolla, MO 65409, USA*

[2]*Department of Biological Sciences, UMR, Rolla, MO 65409, USA*

## ABSTRACT

An intelligent microfluidic system with oxidase enzyme coupled biosensors. Baseline (zero-value) drift and sensitivity degradation are two common problems related with biosensors. In order to overcome these problems, there is a great need for integrating an on-demand, *in situ* self-diagnosis and self-calibration unit along with the sensor. Utilizing the microfluidic technology, the feasibility of implementing this function is implemented without any externally coupled bulky apparatus. A microsystem including a microfluidic channel and calibration electrodes are prepared by microfabrication techniques. A novel method of using hydrogen and oxygen bubbles generated by electrolysis of water is used to saturate the solution with these gases in the microfluidic channel where the biosensor is placed. The hydrogen bubble provides oxygen-depleted microenvironment to conduct a zero-value calibration procedure for the sensor. The oxygen bubble provides high sensitivity and constant oxygen background environment to allow stable enzyme reactions that is not limited or perturbed by the fluctuation of background oxygen in sample solutions. Commercial oxygen sensors and pH sensors are used to confirm whether saturation or depletion of oxygen has occurred with minimum local pH change near the sensor during the electrolytic bubble generation. The glucose data obtained from the experiments assure that the proposed method is promising to overcome the above mentioned two problems.

*Keywords:* bubble, electrolysis, calibration, oxygen, hydrogen, glucose.

## 1. INTRODUCTION

The two main problems which biosensors exhibit are baseline drift and sensitivity degradation. This calls for an *in situ* self-diagnosis and self-calibration procedure that helps to improve the overall functioning of the biosensor. The basic motive is to manipulate the oxygen microenvironment around the sensor. By performing electrolysis of water, it is possible to generate either a hydrogen bubble or oxygen bubble. The hydrogen bubble provides oxygen-depleted microenvironment to conduct a zero-value calibration procedure for the sensor since the enzyme reaction cannot be completed without oxygen. On the other hand, the oxygen bubble helps in increasing the dynamic range and sensitivity of the sensor by providing constant oxygen-saturated environment. The reactions occurring at the anode and cathode of the calibration electrode pair are as follows:

$2H_2O \rightarrow 4H^+ + 4e^- + O_2$ (anode)

$4H_2O + 4e^- \rightarrow 4OH^- + 2H_2$ (cathode)

The above reactions create either oxygen saturated or depleted environment around the biosensor [1], [2].

Glucose detection is based on the amperometric detection of hydrogen peroxide caused by the oxidation of glucose (ß-D-Glucose) catalyzed in the presence of glucose oxidase (GOD) enzyme. The reaction is as follows:

$$\text{ß-D-Glucose} + O_2 \xrightarrow{\text{GOD}} \text{Gluconic acid} + H_2O_2$$

The detection of hydrogen peroxide is amperometrically done by the working electrode of glucose sensor which is biased positive (0.8V) with respect to the reference electrode. The above reaction shows the oxygen dependency of enzyme reaction. The enzyme catalyses the conversion of glucose to gluconic acid and hydrogen peroxide in the presence of oxygen. When a hydrogen bubble is generated and shifted towards the location of the glucose biosensor, the oxygen-depleted environment prevents the enzyme reaction to take place. This mimics a glucose-free environment even in the presence of glucose in sample solutions and provides the environment for zero-value calibration. On the other hand, when an oxygen bubble is generated and shifted, the environment around the sensor is saturated with oxygen for enzyme reaction and is thus not limited by the oxygen availability in the solution. This also helps in sensitivity enhancement because the enzyme reaction is not limited by oxygen. The increased sensitivity due to the oxygen bubbles effectively suppresses the noise ratio caused by electrochemical interferents.

In the previous method of *in situ* calibration [3], the hydrogen and oxygen bubbles which were used for zero-value calibration and sensitivity enhancement were generated remotely from the sensor. Then the bubble was shifted below the biosensor placed in a microfluidic channel in such a way that the biosensor was completely surrounded by the respective bubble. Tests based on this procedure sometimes showed inconsistent and erroneous results. It was considered that the most possible reason for this was that the bubbles were drying up the enzyme layer located at the biosensor tip during the calibration phase. This suggested that a modification to the calibration technique was required.

The new method of calibration involves generating hydrogen or oxygen bubbles relatively close to the sensor and shifting the respective bubble short distances towards the sensor and then stopping the bubble in proximity to the sensor such that it does not touch the sensor tip but saturates or depletes oxygen close to the sensor. Also, the water electrolysis inevitably accompanies a pH change. The enzyme activity changes with respect to pH. Therefore, significant pH changes during bubble generation had to be minimized near the sensor. For this method to be put in to effect several parameters needed to be optimized in the channel design. The parameters are 1) final distance between bubble and sensors following shifting after bubble generation and 2) current density for electrolysis. Experiments were setup using a commercial pH sensor and an oxygen sensor to arrive at the optimum value of the parameters stated above to saturate or deplete oxygen near the sensor, yet to minimize pH change. Chronoamperometric tests were carried out with the modified calibration technique for the biosensor placed in microfluidic channel.

## 2. EXPERIMENTS

### 2.1. Chip design and fabrication

The chip contains a cover layer, an electrode substrate and the necessary sensor probe (pH, oxygen, or glucose sensor) as in Figure 1(a). Initially a mask was designed with the required channel patterns. The channel width was 1mm at the extremes and 0.5mm at the point of the sensor entry. A silicon wafer with silicon nitride layer coating was used as the electrode substrate. A pair of oxygen and hydrogen bubble was generated by a pair of platinum counter electrode and calibration electrode in the substrate. Bubble

stoppers were placed at the required distances so that the final distances between the sensor and bubble (from calibration electrode), post bubble generation stood at 5mm, 3mm, and 1mm , respectively, after bubble shifting as shown in Figure 1(b), 1(c), and 1(d).

The mask image was then transferred to a negative photoresist (MicroChem, SU-8) spin-coated on a silicon wafer using the photolithography techniques. The height of the patterns on the silicon wafer was obtained as 150μm using triple coating of the photoresist. The cover layer was made of polydimethylsiloxane (PDMS). The silicon wafer with the patterns on it was used as a template for molding process of PDMS. The curing of one cm thick PDMS was done for 24h at room temperature in a vacuum desiccator. The PDMS cover layer was now aligned on the substrate so that the electrode pairs were exposed within the channel. The sealing between them was done by simply pressing the cover layer against the substrate. A small hole was drilled to insert sensors (pH, oxygen or glucose) in the PDMS cover layer.

**2.2. Sensor preparation and calibration**

The three sensors used in the experiments were oxygen sensor, pH sensor, and glucose sensor. The oxygen sensor used was a needle type fiber optic sensor (WPI, OxyMicro) with a fiber diameter of 125μm. Two-point calibration of the oxygen sensor was done by bubbling oxygen gas or nitrogen gas through DI water separately for 15 mins. This represented 100% and 0% oxygen saturation that formed the two points of calibration. The gases were provided using two mass flow controllers (MKS instruments, 1159B). The required flow was chosen from a 4-channel readout power supply (MKS

Instruments, 247C). The pH sensor used was AMANI (Innovative Instruments Inc.) of tip diameter of 0.45mm with a detecting unit (Orion EA 940). For the pH sensor three-point calibration was done by using three buffer solutions of pH 4, pH 7 and pH 10. For the preparation of the wire type glucose sensor, glutaraldehyde, glucose oxidase (GOD) and bovine serum albumin (BSA) were used. All were obtained from Sigma (Sigma Chemical Co., St. Louis, MO). Phosphate buffer (PB) was used for dissolving GOD and BSA. A Teflon-coated platinum (Pt) wire was used as working electrode and a chloridated silver tube (AgCl) acted as the reference electrode for the sensor. The Pt wire was inserted into the Ag tube to make a completed sensor assembly. The teflon layer served as an insulation layer between the two electrodes. Triethoxysilane (1 wt %) was deposited on the electrode surface and was cured for 30 mins at 80$^{o}$C. Then GOD and BSA were mixed in PB in the ratio of 1.0:5.0 and the mixture was transferred to the exposed distal tip of Pt electrode. It was cured for 30 mins at room temperature. Then glutaraldehyde (5 wt %) which was used for crosslinking was transferred to the sensor tip as a final step and cured for 30 mins at room temperature. The whole sensor assembly was then kept in PB for 24 h before use. The glucose solutions were prepared by mixing the appropriate quantities of glucose (ß-D-Glucose) in PB.

**2.3. Measurement**

For performing the electrolysis of water to generate bubbles, an electrochemical instrument (Gamry Instruments, FAS1) was operated in chronopotentiometric mode (i.e. constant current). To observe and record the processes, a microscope equipped with a CCD camera (Nikon DS-L1) was used. Once the bubble was generated it was shifted so

that the final distance between the bubble and sensors stood as 5mm, 3mm and 1mm. Current densities of 3.5, 5.5, 7.5, and 12.0mA/cm$^2$ were chosen. These values were assumed to give negligible pH changes and maximum oxygen saturation or depletion state in proximity to the sensor. Experiments were conducted with the pH sensor and oxygen sensor. The bubble was generated for 2 mins by applying each current density and was shifted until it was stopped by the bubble stopper. The readings were analyzed to find the optimum distance between the bubble and sensor and the current density that needed to be applied. Once the optimum values were fixed, glucose measurements were done by biasing the sensor working electrode at 0.8V with respect to reference electrode using the chronoamperometric mode (i.e. constant voltage) of the electrochemical instrument (Gamry Instruments, FAS1). The different glucose concentrations chosen were 0, 50, 100, 200, 300 mg/dl. Two types of glucose concentration measurements were done. In the first type the chronoamperometric response of a glucose sensor for different glucose concentrations was measured with the glucose solutions in a 50ml beaker saturated or depleted of oxygen. In the second type the chronoamperometric response was measured with the glucose solution saturated or depleted of oxygen by bubbles within the microfluidic channel. In the latter case, the bubble was generated for 2 mins at optimized current density and the measurement was taken after 30secs.

## 3. RESULTS AND DISCUSSION

### 3.1. pH sensor

As can be seen from Figure 2(a) for final distance between the bubble and pH sensor as 5mm (i.e. no shifting) during the hydrogen bubble generation phase, the pH increases by a very small amount for minimum current density of 3.5 mA/cm$^2$ and by a

large amount (up to 8.1) for the maximum current density of 12 mA/cm$^2$. For oxygen bubble, the pH decreases by a very small amount for minimum current density and by a large amount (down to 6.7) for the maximum current density. After the bubble generation phase, the pH remains almost constant and recovers to the original pH of glucose solution very slowly. Figure 2(b) and 2(c) shows the same set of curves obtained for final distance between the bubble and pH sensor as 3mm and 1mm, respectively, after bubble shifting. As expected during the bubble generation phase, the general trend of the respective curves was to go up for hydrogen and down for oxygen. But the recovery to original pH after the bubble shifting was much faster. From Figure 3(a), 3(b) and 3(c), it is evident that closer the bubble is to the sensor (1mm), quicker is the stabilization of the pH to its nominal value (about 30 secs).

### 3.2. Oxygen sensor

Figure 3(a) represents the time response of oxygen saturation percentage for final distance between sensor and bubble as 5mm. The plots show that the percentage of oxygen saturation remains at 21% (both oxygen and hydrogen) for all the current densities when no shifting of bubble has taken place after the bubble generation phase. The bubble generated at maximum distance of 5mm from the sensor is not effective at all to cause saturation or depletion of oxygen near the sensor. Figure 3(b) shows the time response for final distance of 3mm after bubble shifting. During the bubble generation phase, the oxygen concentration remains almost at 21% for all the current densities. After the respective shifting, however, it is seen that for minimum current density of 3.5mA/cm$^2$, the oxygen saturation and depletion are approximately 30% and 11%,

respectively. For maximum current density of 12mA/cm$^2$ used, the oxygen saturation and depletion are approximately 90% and 10%, respectively. In Figure 3(c) for the final distance of 1mm, for all current densities except the lowest one, the respective oxygen saturation and depletion percentages stand at around 95% and 5%, respectively. Many facts were confirmed from the oxygen saturation and depletion curves. As expected, the higher the current density used, the better is the oxygen saturation or depletion. The closer the bubble is to the sensor, the higher is the oxygen saturation or depletion. From Figure 3, it is evident that a current density that causes minimum pH variation with maximum oxygen saturation or depletion states and minimum distance between the bubble and sensor has to be chosen. The best condition is 5.5mA/cm$^2$ with a final distance as 1mm. For this case it was found that the oxygen saturation and depletion were 93% and 5%, respectively. The PDMS material used for the cover layer has high oxygen permeability. This material was used however, because of its elasticity to allow the sensor probes to be mounted in the cover layer with ease.

### 3.3. Glucose sensor

Figure 4 represents the chronoamperometric responses for the two types of glucose measurement approaches that were considered. Figure 4(a) shows the response for a fixed glucose concentration of 300mg/dl with three different oxygenation states in a beaker. They are nitrogen saturated, air-saturated, and oxygen saturated states. Figure 4(b) shows the response for the same fixed glucose concentration of 300mg/dl with the different oxygenation conditions achieved by electrolyzed bubble method. The final distance between sensor and bubble and current density were optimized as 1mm and

5.5mA/cm$^2$ within the fluidic chip based on the pH and oxygen measurment. It was noted that both the approaches gave very similar results. Figure 5(a) and 5(b) compares the current versus variable glucose concentration plot for the two types of measurement approaches. It is evident that during the hydrogen bubble phase the signal is almost constant regardless of the existing glucose concentration, which is promising to realize periodic, *in situ*, self-calibration of zero-value correction procedures. With the oxygen bubble, the sensitivity is higher than that of air-saturation solution.

## 4. CONCLUSION

An amperometric glucose sensor with a novel method of one-point, *in situ*, on demand, self-calibration has been presented. The bubble was brought close to the sensor so that the glucose solution in proximity to the sensor is saturated or depleted of oxygen with minimum pH perturbation. Bubble shifting was required after bubble generation. The optimum value of final distance between bubble and sensor and current density to be applied were investigated by setting up requisite experiments with pH sensor and oxygen sensor. The use of a channel material with lower oxygen permeability other than PDMS will improve the device performance is expected.

## REFERENCES

[1] C.S. Kim, C. Lee, J. O. Fiering, S. Ufer, C. W. Scarantino, and H. T. Nagle, "Manipulation of microenvironment with a built-in electrochemical actuator in proximity of a dissolved oxygen microsensor," *IEEE Sensors Journal*, Vol.4, No.5, pp. 568-575, October 2004.

[2] J. Park, C.S. Kim, and Y. Kim, "A simple on-chip self-diagnosis/self-calibration method of oxygen microsensor using electrochemically generated bubbles," *Sensors and Actuators B, Chem.*, Vol.108, No.1-2, pp. 633-638, 2005.

[3] J. Park, C.S. Kim, and M. Choi, “Oxidase-Coupled Amperometric Glucose and Lactate Sensors with Integrated Electrochemical Actuation System,” *IEEE Transactions on Instrumentation and Measurement*, Vol. 55, No. 4, pp. 1348-1355, August 2006.

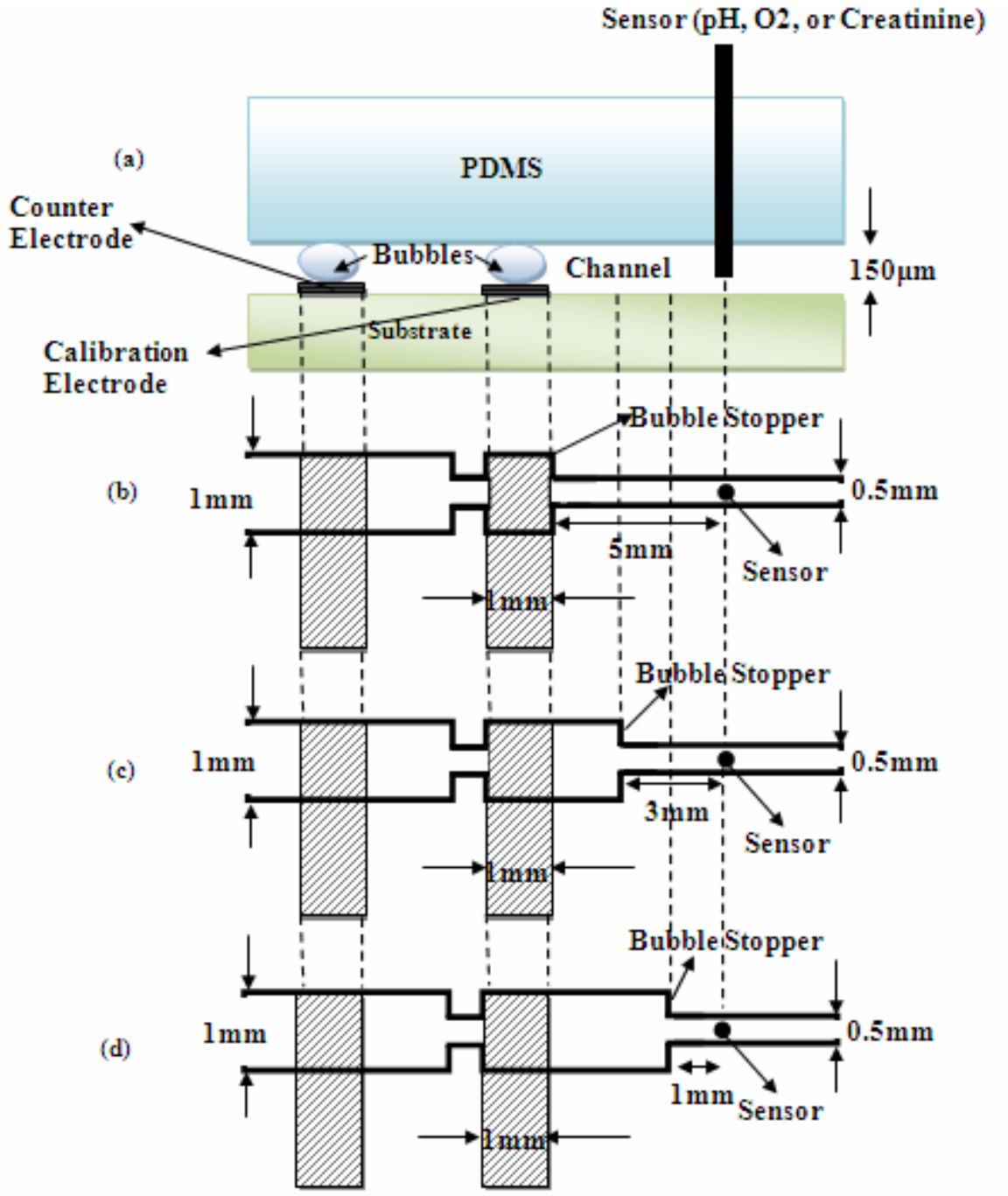


Figure 1. Side view and three different channel layouts. The bubble is generated and shifted towards bubble stopper (a) Side view of fluidic chip. (b) Top view of the channel pattern for final distance of 5mm (i.e. no shifting). (c) final distance of 3mm. (d) final distance of 1mm.

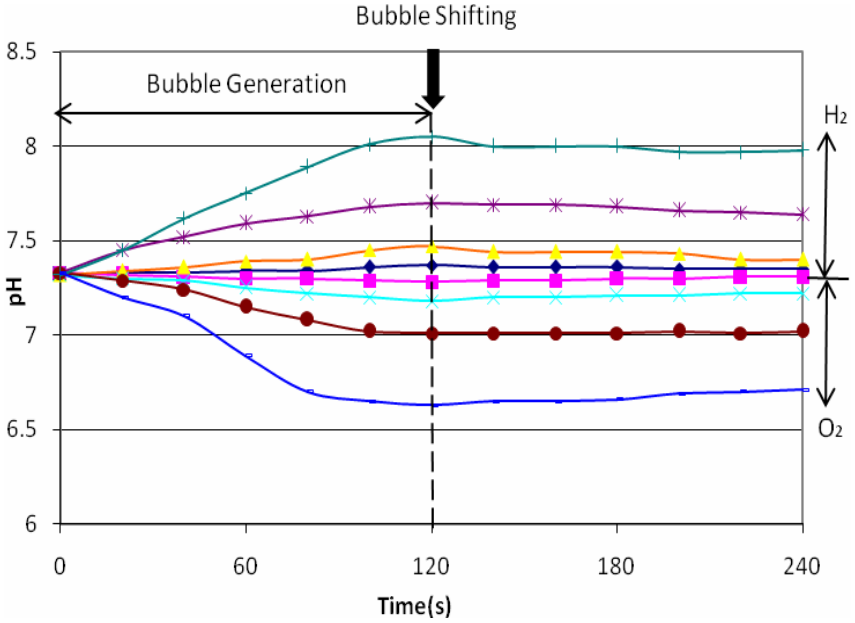


(a) final distance of 5mm (i.e. no shifting).

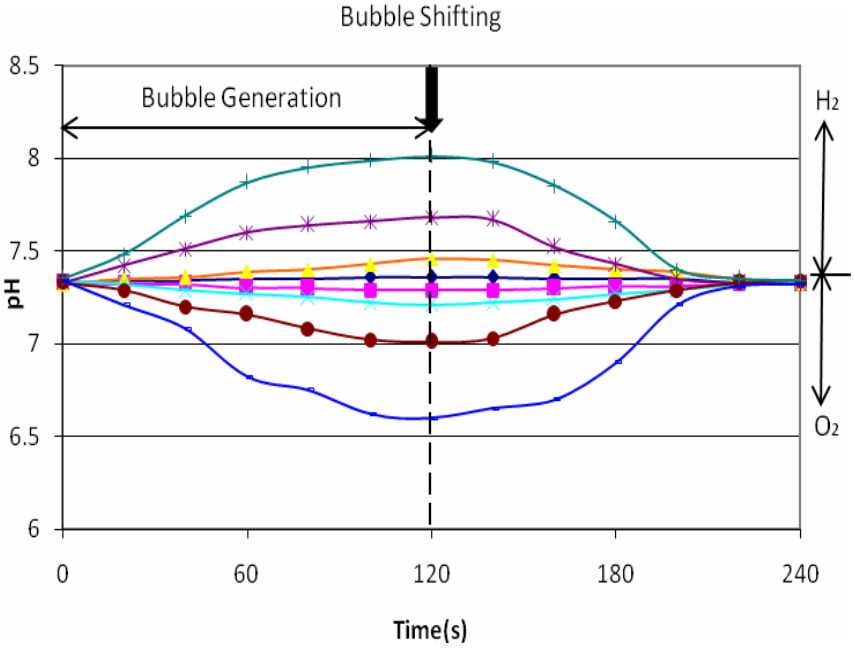


(b) final distance of 3mm.

Figure 2. Responses of pH sensor for different distances between bubble and sensor, post bubble generation for 2 mins and shifting, at current densities of 3.5, 5.5, 7.5, 12.0mA/cm$^2$.

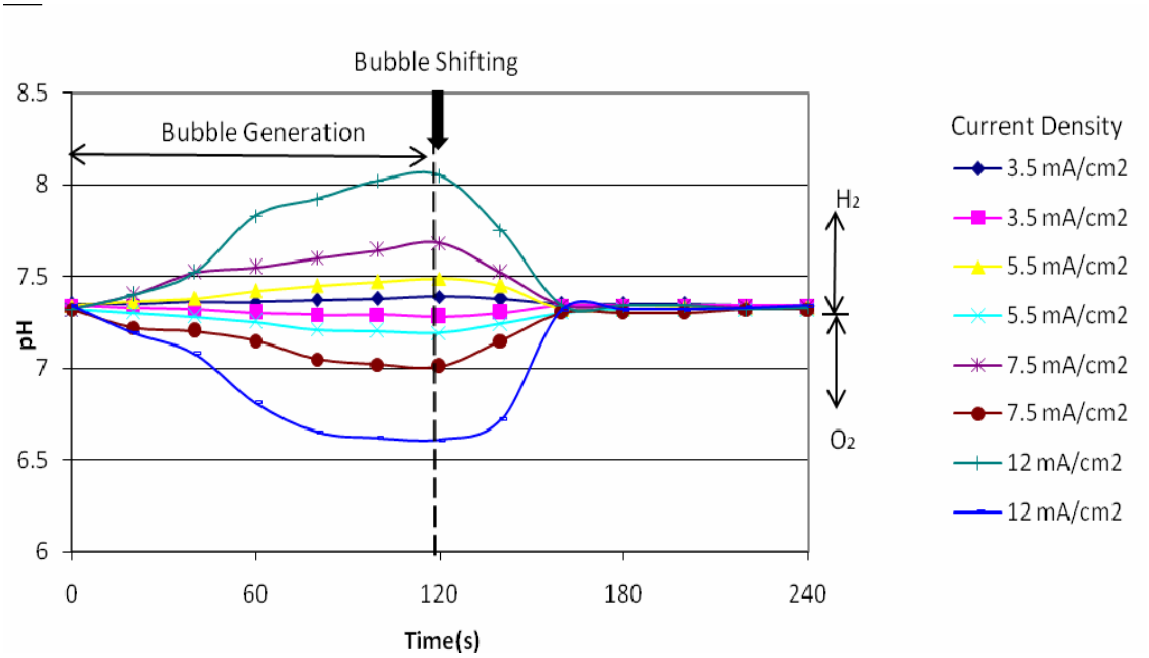


(c) Response for final distance of 1mm.

Figure 2. (Continued) Responses of pH sensor for different distances between bubble and sensor, post bubble generation for 2 mins and shifting, at current densities of 3.5, 5.5, 7.5, 12.0mA/cm$^2$.

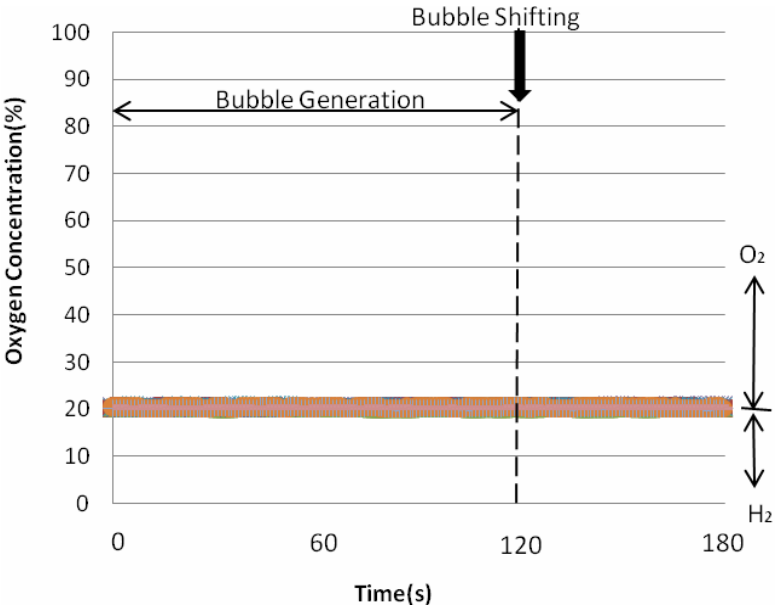


(a) final distance of 5mm(i.e. no shifting).

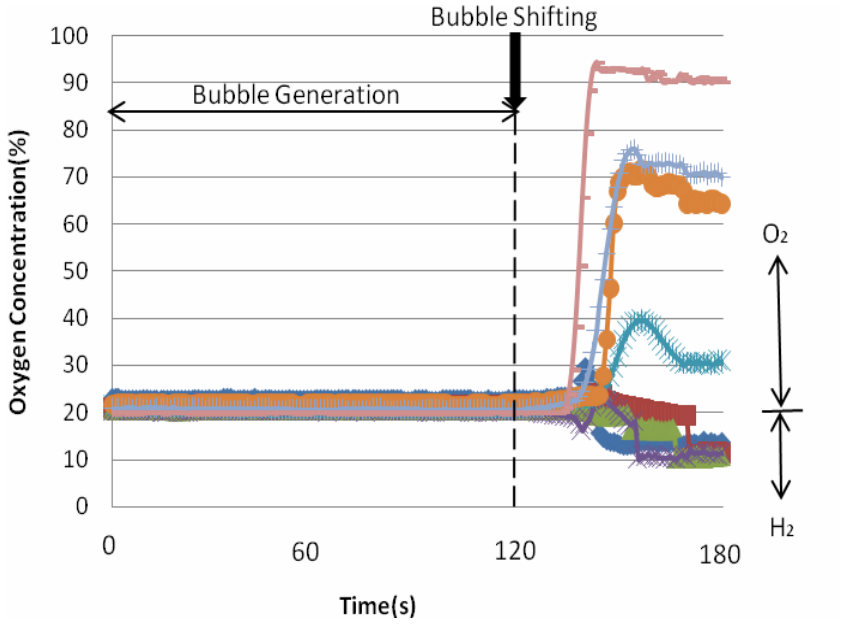


(b) final distance of 3mm.

Figure 3. Responses of oxygen sensor for different distances between bubble and sensor, post bubble generation for 2 mins and shifting, at current densities of 3.5, 5.5, 7.5, 12.0mA/cm$^2$.

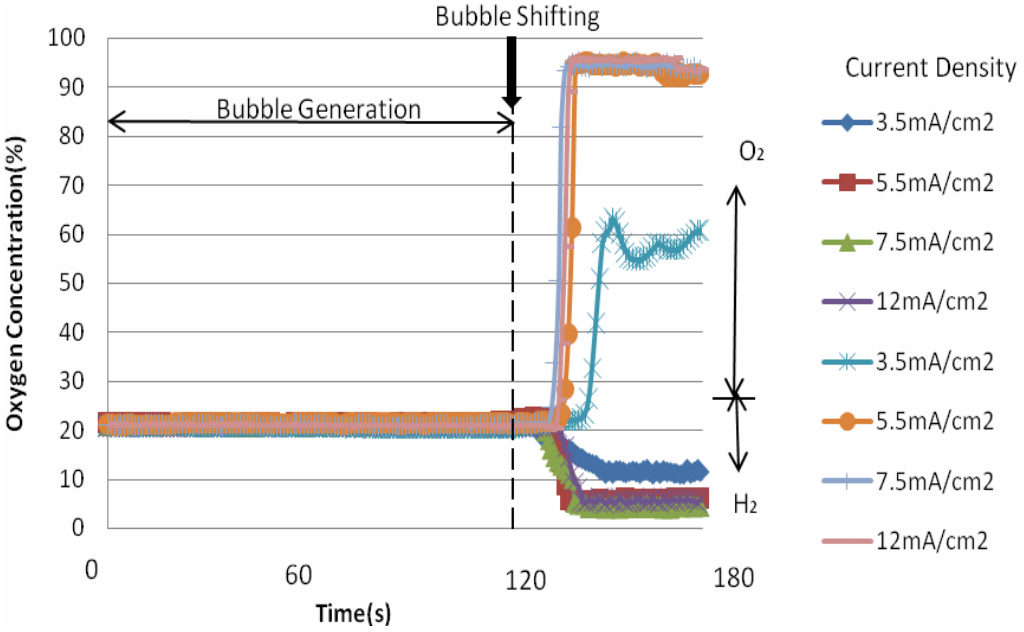


(c) Response for final distance of 1mm.

Figure 3. (Continued) Responses of oxygen sensor for different distances between bubble and sensor, post bubble generation for 2 mins and shifting, at current densities of 3.5, 5.5, 7.5, 12.0mA/cm$^2$.

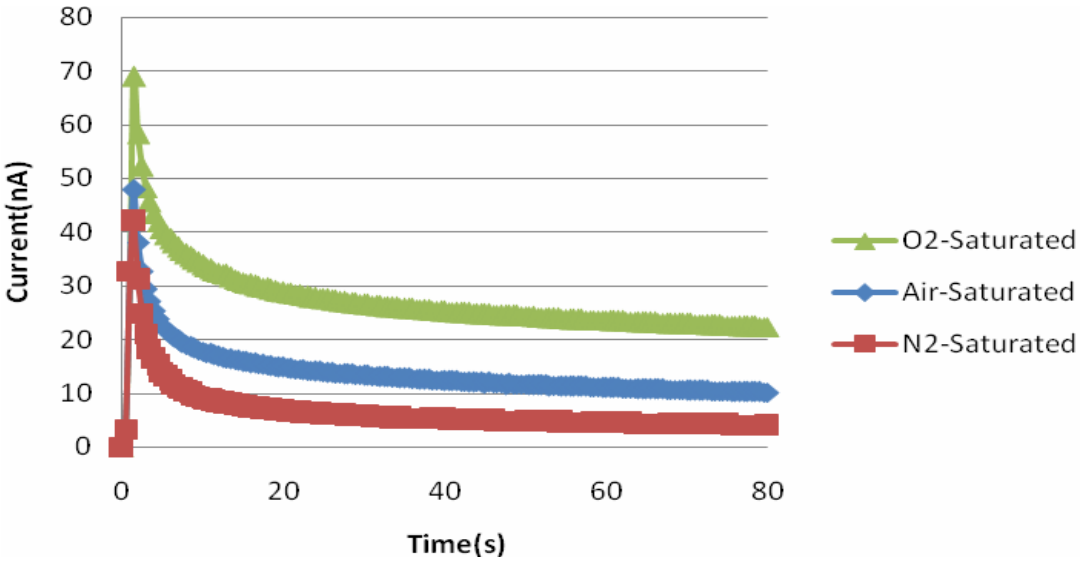


(a) Response with sensor placed in glucose solutions saturated or depleted of oxygen by bubbling oxygen or nitrogen in a beaker.

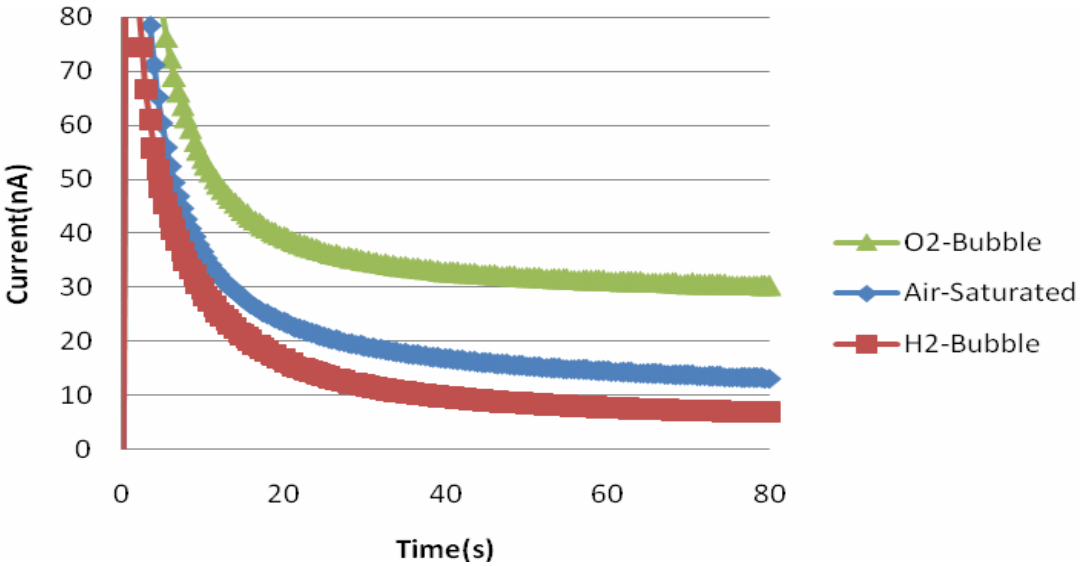


(b) Response within the chip when glucose solution saturated or depleted by bubbles in microfluidic channel at optimized final distance and current density.

Figure 4. Chronoamperometric time responses of the glucose sensor for a fixed concentration of 300mg/dl.

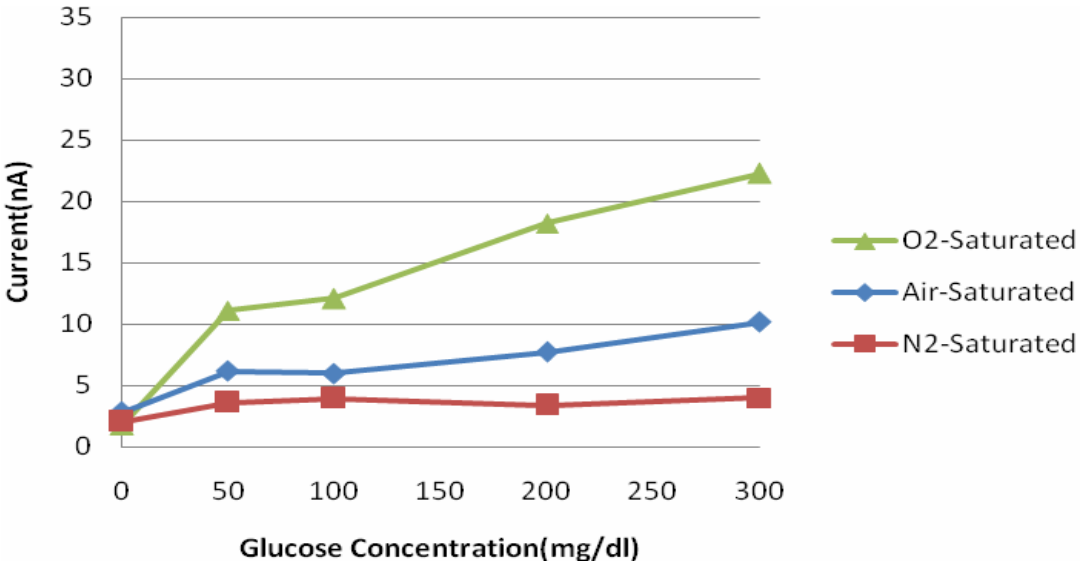


(a) Plot with sensor placed in glucose solutions saturated or depleted of oxygen by bubbling oxygen or nitrogen in a beaker.

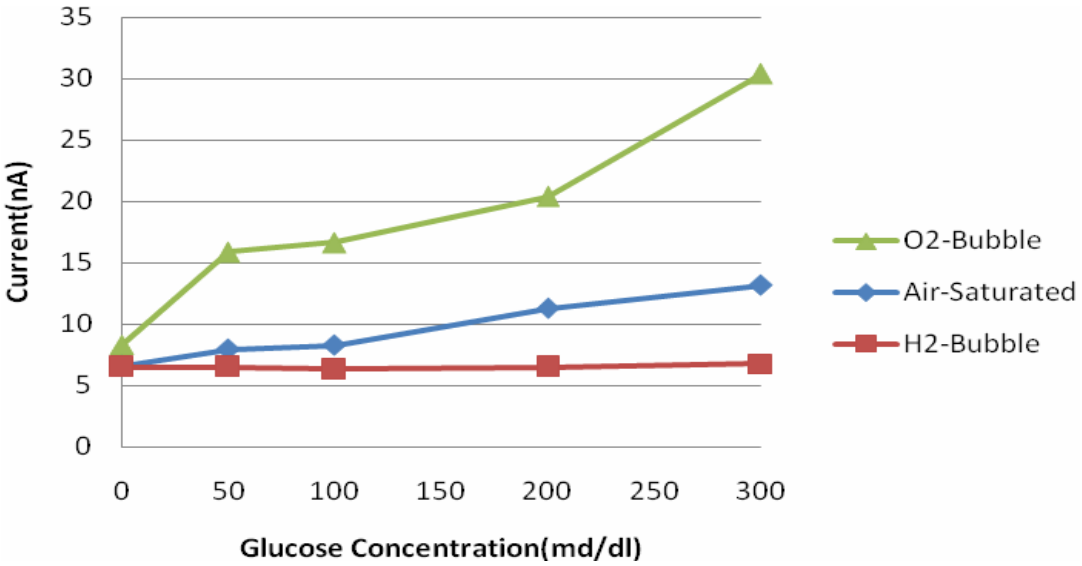


(b) Plot within the chip when glucose solution saturated or depleted by bubbles in microfluidic channel at optimized final distance and current density.

Figure 5. Glucose concentration versus current plot.

# An intelligent microfluidic creatinine biosensor

Nitin Radhakrishnan[a], Jongwon Park[a], Chang-Soo Kim[a,b]
[a]Department of Electrical & Computer Engineering, UMR, Rolla, MO 65409, USA
[b]Department of Biological Sciences, UMR, Rolla, MO 65409, USA

## ABSTRACT

An intelligent microfluidic system for creatinine determination with a tri-enzyme based detection scheme is described. Creatinine amidohydrolase (CA), creatine amidinohydrolase (CI) and sarcosine oxidase (SO) are used to detect creatinine amperometrically. The two most common problems with biosensors are baseline (zero-value) drift and sensitivity degradation. In order to circumvent these problems, there is a great need for integrating an on-demand, *in situ*, self-diagnosis and self-calibration unit along with the sensor. Utilizing the microfluidic technology, it is possible to explore the feasibility of implementing this function without any externally coupled bulky apparatus. Electrolysis of water is done to generate hydrogen and oxygen bubbles. These bubbles are used to saturate the solution close to biosensor in a microchannel. The hydrogen bubble provides oxygen-depleted microenvironment to conduct a one-point (zero-value) calibration procedure for the sensor. The oxygen bubble provides high sensitivity and constant oxygen environment to allow stable enzyme reactions that is not limited or perturbed by the fluctuation of background oxygen in sample solutions. Amperometric signal amplification by oxygen bubble improves the electrochemical signal-to-noise ratio in presence of an interferent (ascorbic acid).

**Keywords**: bubble, electrolysis, calibration, oxygen, hydrogen, creatinine.

## 1. INTRODUCTION

The creatinine level in human blood or serum is a very important clinical parameter in estimating renal, muscular, and thyroid functions. Normal range of creatinine is 0.4 – 1.6mg/dl in adults[1]. Higher creatinine level in blood serum is considered harmful indicating less absorption of them by kidney, while low creatinine level indicates an efficient, effective and healthy pair of kidneys. A value of 11.0mg/dl or more represents an abnormal range[2]. The development of reliable and high-sensitivity creatinine sensors is one of the most challenging tasks in the clinical diagnostic field due the presence of very low creatinine in physiological conditions[3].

Creatinine can be detected both potentiometrically and amperometrically. The former method of detection involves the use of enzyme(s) that catalyses the conversion of creatinine to ammonia. This is detected by an ion or gas sensitive electrode or an ion sensitive field effect transistor (ISFET)[4,5,6,7] that give results as a variation of pH. The interference from the ammonium ions and other cationic species in blood plasma and urine, low detection limit of creatinine are issues which have to be considered in this method of detection. This method is complicated owing to the use of pH electrodes to measure creatinine.

The amperometric scheme is simple and makes use of simple thin film electrodes that do not require pH electrode to detect creatinine. This method which is widely accepted involves the use of a tri-enzyme matrix membrane. Three enzymes namely creatinine amidohydrolase (CA), creatine amidinohydrolase (CI) and sarcosine oxidase (SO) are used to detect creatinine. These enzymes help to sequentially convert creatinine to creatine and finally, to sarcosine and hydrogen peroxide[8,9,10,11,12,13,14]. The two main

factors which have to be considered here are the efficient coupling between the enzymes and significant creatinine response current. The enzymes, bovine serum albumin (BSA) and phosphate buffer (PB) are normally used for making the tri-enzyme matrix. The choice of the ratio between them has to be carefully selected to provide higher sensitivity to low creatinine level. The interference posed by creatine can be reduced by careful selection of the ratio between the enzymes[14]. The reactions in the tri-enzyme matrix are as given below:

$$\text{Creatinine} + H_2O \xrightarrow{CA} \text{Creatine} \quad [1]$$

$$\text{Creatine} + H_2O \xrightarrow{CI} \text{Sarcosine} + \text{Urea} \quad [2]$$

$$\text{Sarcosine} + H_2O + O_2 \xrightarrow{SO} \text{Glycine} + \text{Formaldehyde} + H_2O_2 \quad [3]$$

The detection of hydrogen peroxide is amperometrically done by the working electrode of creatinine sensor which is biased positive (0.8V) with respect to the reference electrode. The above reaction shows the oxygen dependency of the enzyme reaction.

The two main problems which biosensors exhibit are baseline drift and sensitivity degradation. Works have been done on *in situ*, on-demand, self-diagnosis and self-calibration procedures that help to improve the overall functioning of the dissolved oxygen sensor and oxidase-based biosensors[15,16,17]. By performing electrolysis of water, generations of either hydrogen bubble or oxygen bubble to manipulate the oxygen microenvironment around the sensor can be done. The reactions occurring at the anode and cathode of an electrolysis electrode pair are as follows:

$$2H_2O \rightarrow 4H^+ + 4e^- + O_2 \text{ (anode)} \quad [4]$$

$$4H_2O + 4e^- \rightarrow 4OH^- + 2H_2 \text{ (cathode)} \quad [5]$$

The hydrogen bubble provides oxygen-depleted microenvironment to conduct a one-point (zero-value) calibration procedure for the sensor since the oxidase reaction cannot be completed without oxygen. On the other hand, the oxygen bubble helps in increasing the dynamic range and sensitivity of the sensor by providing constant oxygen-saturated environment. In the previous method of one-point, *in situ,* self-calibration[17], the hydrogen and oxygen bubbles were shifted below the biosensor placed in a microfluidic channel in such a way that the biosensor tip was completely surrounded by the respective bubble. Tests based on this procedure sometimes showed inconsistent and erroneous results. It was considered that the bubbles were drying up the enzyme layer located at the biosensor tip during the calibration phase. Another possible reason is that the reaction byproducts accumulate within the enzyme layer since it is disconnected from the bulk solution by the surrounding bubble. This suggested that an improvement to the calibration technique was required.

The new method of calibration involves generating hydrogen or oxygen bubbles relatively close to the sensor and shifting the respective bubble short distances towards the sensor. The bubbles are then stopped by a bubble stopper in proximity to the sensor such that it does not touch the sensor tip but saturates or depletes oxygen close to the sensor. The water electrolysis inevitably accompanies a pH change as in reactions [4] and [5], which may change enzyme activity. Therefore, the pH change during bubble generation has to be minimized near the sensor. For this method to be put in to effect, important parameters needed to be optimized. The parameters are 1) final distance between bubble and sensors following shifting of bubble and 2) current density for electrolysis. Experiments were setup using a commercial pH sensor and an oxygen sensor

to arrive at the optimum value of the parameters stated above to saturate or deplete oxygen near the sensor, yet to minimize pH change. Then chronoamperometric tests were carried out with the modified calibration technique for the creatinine biosensor placed in microfluidic channel.

## 2. EXPERIMENTS

### 2.1 Chip design and fabrication

The chip contains a cover layer, an electrode substrate and the necessary sensor probe (pH, oxygen, or creatinine sensor) as in Figure 1(a). The cover layer was made of polydimethylsiloxane (PDMS) containing the necessary channel patterns. The channel width was 1mm at the extremes and 0.5mm at the point of the sensor entry. A silicon wafer with silicon nitride layer coating was used as the electrode substrate. A pair of oxygen and hydrogen bubble was generated by a pair of platinum counter electrode and calibration electrode on the substrate. Bubble stoppers were placed at the required distances so that the final distances between the sensor and bubble stood at 5mm, 3mm, and 1mm, respectively, after bubble shifting as shown in Figure 1(b), 1(c), and 1(d).

For the fabrication of the electrodes, a platinum/titanium thin film (100nm/20nm) was deposited by e-beam evaporation and patterend by lift-off technique to define the electrodes. A PDMS channel height of at least 150μm was necessary to locate the sensor distal tip at the middle of the channel by inserting it manually. To achieve this, triple coating of a photoresist was needed. A recipe for this was properly formulated. The steps involved in the fabrication are shown in Figure 2. A silicon wafer was first subjected through a three step cleaning process involving acetone, methyl alcohol and deionized

(DI) water. The first layer of photoresist was spin-coated at 1000 rpm on the silicon wafer. The photoresist used was of negative tone, high aspect ratio, and epoxy-based photopolymer (SU-8 2050, MicroChem). This was now subjected to soft baking times of 5 mins and 30 mins at temperatures of 65$^{o}$C and 95$^{o}$C, respectively. The second layer of SU-8 was spin-coated at 1000 rpm on the existing soft baked first layer. Soft baking times of 7 mins and 45 mins at temperatures of 65$^{o}$C and 105$^{o}$C were chosen. Finally, the third layer was spin coated and baked as the same condition with the second layer. The pattern on the photomask was transferred to the SU-8 by exposing it with UV rays. The wafer was now subjected to post baking times of 5 mins and 15 mins at temperatures of 65$^{o}$C and 95$^{o}$C. Finally, the unexposed parts of SU-8 were removed by putting it in a developer solution for 15 mins. The silicon wafer with channel patterns could now be used as a template for the molding process of the PDMS (Sylgard, Dow Corning) cover layer. The curing of one cm thick PDMS was done for 24h at room temperature in a vacuum desiccator.

**2.2 Creatinine sensor preparation**

For the preparation of the wire type creatinine sensor, glutaraldehyde, creatininase (CA), creatinase (CI), sarcosine oxidase (SO) and BSA were used. All were obtained from Sigma (Sigma Chemical Co.,). Phosphate buffer (PB, pH 7.4, 10mM) was prepared by mixing $NaH_2PO_4$ and $KH_2PO_4$ and was used for dissolving CA, CI, SO, and BSA. Creatinine and ascorbic acid were also obtained from Sigma (Sigma Chemical Co.,). A teflon-coated platinum (Pt) wire (A-M Systems, Inc.) with a diameter of 0.008” was used

as working electrode and a chloridated silver (Ag) tube (GoodFellow) with an inner diameter of 0.3mm acted as the reference electrode for the sensor.

The Pt wire was inserted into the Ag tube to make a two-electrode amperometric sensor. The teflon layer served as an insulation layer between the two electrodes. Triethoxysilane (1 wt %) was deposited on the distal tip of this coaxial electrode and was cured for 30 mins at 80$^{o}$C. The ratio between the enzymes (CA: CI: SO) was chosen such that there was significant response current for creatinine with minimum interference from creatine[14]. Then the tri-enzyme mixture (CA, CI, SO) and BSA were mixed in the weight ratio of 1.0:5.0. This ratio was carefully selected so as to provide high sensitivity for low creatinine levels. Finally, the mixture was dissolved in PB in the weight ratio of 1.00:5.67. The enzyme solution was transferred to the exposed distal tip of Pt electrode and dried for 30 mins at room temperature. Then glutaraldehyde (5 wt %) which was used for crosslinking was transferred to the sensor tip as a final step and cured for another 30 mins at room temperature. The whole sensor assembly was immersed in PB and then kept in refrigerator for 24 h before use. The creatinine solutions were prepared by mixing the appropriate quantities of creatinine in PB. A known quantity of ascorbic acid was added to one of the creatinine solution concentrations.

**2.3 Measurement**

The PDMS cover layer was aligned on the substrate so that the electrode pairs were exposed within the channel. The sealing between them was done by simply pressing the cover layer against the substrate. A small hole was drilled to insert needle type sensors (pH, oxygen or creatinine) in the PDMS cover layer. The oxygen sensor used was

a needle type fiber optic sensor (OxyMicro, WPI) with a fiber diameter of 125µm. Two-point calibration of the oxygen sensor was done by bubbling oxygen gas or nitrogen gas through DI water separately for 15 mins before use. This represented 100% and 0% oxygen saturation that formed the two points of calibration. The gases were provided using two mass flow controllers (1159B, MKS instruments). The required flow was chosen from a 4-channel readout power supply (247C, MKS Instruments). The pH sensor (AMANI, Innovative Instruments Inc.) has tip diameter of 0.45mm with a detecting unit (EA 940, Orion). For the pH sensor, three-point calibration was done by using three buffer solutions of pH 4, pH 7 and pH 10 before actual use.

For performing the electrolysis of PB to generate bubbles, an electrochemical instrument (FAS1, Gamry Instruments) was operated in chronopotentiometric mode (i.e. constant current). To observe and record the processes, a microscope equipped with a CCD camera (DS-L1, Nikon) was used. Once the bubble was generated it was shifted so that the final distance between the bubble and sensors stood as 5mm, 3mm and 1mm. Current densities of 3.5, 5.5, 7.5, and 12.0mA/cm$^2$ were chosen. These values were assumed to give negligible pH changes and maximum oxygen saturation or depletion state in proximity to the sensor. Experiments were conducted with the pH sensor and oxygen sensor. The bubble was generated for 2 mins by applying each current density and was then shifted by applying pressure from the left side of the channel in Figure 1. It was almost instantaneously stopped by the bubble stopper. The readings were analyzed to find the optimum distance between the bubble and sensor and the current density for electrolysis.

Once the optimum values were fixed, creatinine measurements were done by biasing the sensor working electrode at 0.8V with respect to reference electrode using the chronoamperometric mode (i.e. constant voltage) of the electrochemical instrument (FAS1, Gamry Instruments). The different creatinine concentrations chosen were 0, 5, 10, 15, 20 mg/dl. Two types of creatinine concentration measurements were done. In the first type the chronoamperometric response of a creatinine sensor for different creatinine concentrations was measured with the creatinine solutions in a 50ml beaker saturated or depleted of oxygen by gas bubbling. In the second type the chronoamperometric response was measured with the creatinine solution saturated or depleted of oxygen by bubbles within the microfluidic channel. In the latter case, the bubble was generated for 2 mins at optimized current density and the measurement was taken after 30secs. An electrochemical signal-to-noise ratio (S/N) test was conducted on creatinine solution concentration of 15mg/dl containing an electrochemical interferent (1mg/dl ascorbic acid).

## 3. RESULTS AND DISCUSSION

### 3.1 pH sensor

Figure 3(a) shows the time responses of a pH sensor for final distance between the bubble and pH sensor as 5mm (i.e. no shifting). During the hydrogen bubble generation phase, the pH increases by a negligibly small amount for minimum current density of 3.5 $mA/cm^2$ and by a large amount (up to 8.1) for the maximum current density of 12.0 $mA/cm^2$. For oxygen bubble, the pH decreases by a large amount (down to 6.7) for the maximum current density. After the bubble generation phase, the changed pH remains

almost constant and recovers to the original pH of creatinine solution very slowly. Figure 3(b) and 3(c) shows the same set of curves obtained for final distance between the bubble and pH sensor as 3mm and 1mm after bubble shifting. As expected the general trend of the respective curves was to go up for hydrogen and down for oxygen. But the recovery to original pH after the bubble shifting was much faster. It is considered that the perturbation of solution expedited the pH buffering process as the bubble shifts. From Figure 3(a), 3(b) and 3(c), it is evident that closer the bubble is to the sensor (1mm), quicker is the recovery of the pH to its original value (about 30 secs).

**3.2 Oxygen sensor**

Figure 4(a) represents the time response of oxygen saturation percentage for final distance between sensor and bubble as 5mm. The plots show that the oxygen saturation remains at 21% for all the current densities when no shifting of bubble has taken place after the bubble generation phase. The bubble generated at maximum distance of 5mm from the sensor is not effective at all to cause any saturation or depletion of oxygen near the sensor. The most plausible explanation for this little response, compared to the pH responses of Figure 3(a), is that a significant portion of generated oxygen stays and nucleates bubbles at the electrode surface rather than simply migrating into the bulk solution. Also the diffusion coefficient of oxygen in water ($2.42 \times 10^{-5}$ $cm^2/sec$) is lower than those of proton ($9.31 \times 10^{-5}$ $cm^2/sec$) and hydroxyl ion ($5.27 \times 10^{-5}$ $cm^2/sec$) [18].

Figure 4(b) shows the time response for final distance of 3mm after bubble shifting. During the bubble generation phase the oxygen concentration remains almost at 21% for all the current densities. After the respective shifting, however, it is seen that for

the lowest current density of 3.5mA/cm$^2$, the oxygen saturation and depletion states, both return to 21% quickly from about 40% and 15%, respectively. This implies that the ineffective small size of bubble with a low current is not enough to change oxygen environment near the sensor. For maximum current density of 12.0mA/cm$^2$ used, the oxygen saturation and depletion reaches approximately 93% and 8%, respectively, which gradually returns to about 80% and 12%. In Figure 4(c) for the final distance of 1mm, for all current densities except the lowest one, the respective oxygen saturation and depletion percentages initially stand at around 92% and 7%, respectively. The recovery is, however, much slower compared to Figure 4(b), which is desirable for this application. The lowest current density of 3.5mA/cm$^2$ still remains ineffective.

Many facts were confirmed from the oxygen saturation and depletion responses. As expected, the higher the current density used, the better is the oxygen saturation or depletion. The closer the bubble is to the sensor, the higher is the oxygen saturation or depletion. For application purposes a current density that causes minimum pH variation with maximum oxygen saturation or depletion states and a minimum distance between the bubble and sensor has to be chosen. From Figure 3 and Figure 4, the optimum condition is 5.5mA/cm$^2$ with a final distance as 1mm. The PDMS material used for the cover layer has high oxygen permeability which means that this material may not the best choice for this application. This material was used however, because of its elasticity to drill a hole and insert the sensor probe in the cover layer with ease.

### 3.3 Creatinine sensor

Figure 5(a) shows the responses for a fixed creatinine concentration of 10mg/dl with three different oxygenation states in a beaker. They are nitrogen-saturated, air-saturated, and oxygen-saturated states created by purging gases. Fig 5(b) shows the response for the same creatinine concentration with the different oxygenation conditions achieved by electrolyzed bubble method. The final distance (between sensor and bubble) and current density were optimized as 1mm and 5.5mA/cm$^2$ based on the pH and oxygen measurements. From Figure 3(c) and 4(c), the best timing to start the chronoamperometric measurement was determined to be 150sec after starting to generate bubbles. After this time, the pH was recovered to its original value while the oxygen change remains almost the same. Figure 5 represents the similar chronoamperometric responses for these two types of creatinine measurement approaches.

Figure 6 shows the average values of three measurements conducted with three creatinine sensors prepared manually by the same procedure on different dates. The error bars indicate the maximum and minimum values. Figure 6(a) and 6(b) compares the current versus creatinine concentration plots for both measurements. It is evident that during the hydrogen bubble phase the signal is almost constant regardless of the creatinine concentration, which is promising to realize on-demand, *in situ*, self-calibration of zero-value correction procedures. When a hydrogen bubble is generated and shifted towards the location of the creatinine biosensor, the oxygen-depleted environment prevents the enzyme reaction to take place. This mimics the creatinine-free environment even in the presence of creatinine in sample solutions and provides the environment for zero-value calibration. With the oxygen bubble, the sensitivity is

dramatically higher than that of air-saturated solution. When an oxygen bubble is generated and shifted, the environment around the sensor is saturated with oxygen. Thus the enzyme reaction is not limited by the oxygen availability in the solution which leads to sensitivity enhancement.

The increased sensitivity due to the oxygen bubbles effectively suppresses the electrochemical noise ratio caused by electrochemical interference. Figure 7(a) shows the chronoamperometric plots of 15mg/dl creatinine with and without 1mg/dl ascorbic acid (electrochemical interferent) in air-saturation case. Figure 7(b) shows the same for an oxygen saturation case created by the bubble in microchannel. The electrochemical S/N ratio increased from 2.1 to 21.4 ([C-B] / [(C+A)-C], see Figure 7). This was improvement by factor of 10. It was found that the tri-enzyme membrane loses its activity quickly during storage in refrigerator for several days. More stable enzyme immobilization method should be developed to be combined with this bubble method to generate viable creatinine sensors. The use of a channel material with lower oxygen permeability other than PDMS will improve the device performance is expected.

## 4. CONCLUSION

An amperometric creatinine sensor with a novel method of self-calibration and signal amplification has been demonstrated utilizing the microfluidic technology. The electrolytically generated bubble was brought close to the sensor so that the solution in proximity to the sensor is saturated or depleted of oxygen with minimum pH perturbation. The optimum value of final distance between bubble and sensor and current density for electrolysis were investigated by setting up requisite experiments with pH

sensor and oxygen sensor. The on-demand, one-point (zero-value), *in-situ*, self-calibration procedure is possible with the hydrogen bubble method regardless of actual presense of creatinine in the sample solution. Oxygen amplification increased sensitivity which in turn improved the electrochemical S/N ratio. This high-sensitivity device is critically important given the very low physiological creatinine levels. This novel bubble method is also applicable to other oxidase-based enzymatic biosensors such as acetylcholine, cholesterol, alcohol and phenol. This method is expected to have a high impact on the continuous monitoring of many substances in medical diagnosis, bioprocess, and environmental areas.

**REFERENCES**

1. Tietz, N. W., Textbook of Clinical Chemistry, 1st ed., Saunders, Philadelphia, pp.1810, 1986.
2. Sena, F.S., Syed, D., McComb, R. B., Clinical Chemisty, Vol. 34, Issue. 3, pp. 594-595, 1988.
3. Meyerhoff, M.E., Clinical Chemistry, Vol. 36, No. 8(B), pp. 1567-1572, 1990.
4. Elmosallamy, M.A.F., Analytica Chimica Acta, Vol. 564, No.2, pp. 253-257, 2006.
5. Pandey, P.C., Mishra, A.P., Sensors and Actuators B, Chem., Vol. 99, Issues. 2-3, pp. 230-235, May 2004.
6. Hassan, S.S.M., Elnemma, E.M., Mohamed, A.H.K., Electroanalysis, Vol. 17, No. 24, pp. 2246-2253, 2005.
7. Campanella, L., Sammartino, M.P., Tomassetti, M., Analyst, Vol. 115, pp. 827-830, June 1990.
8. Tsuchida, T., Yoda, K., Clinical Chemistry, Vol. 29, No. 1, pp. 55-55, 1983.
9. Madaras, M.B., Buck, R.P., Analytical Chemistry, Vol. 68, No.21, November 1996.

10. Erlenkotter, A., Fobker, M., Chemnitius, G.C., Analytical and Bioanalytical Chemistry, Vol. 372, No.2, pp. 284-292, 2002.

11. Nguyen, V.K., Wolff, C.M., Seris, J.L., Schwing, J.P., Analytical Chemistry, Vol. 63, No. 6, pp. 611-614, 1991.

12. Madaras, M.B., Popescy, I.C., Ufer, S., Buck, R.P., Analytica Chimica Acta, Vol. 319, No.3, pp.335-345, 1996.

13. Yamato, H., Ohwa, M., Wernet, W., Analytical Chemistry, Vol. 67, pp. 2776-2780, 1996.

14. Khan, G. F., Wernet, W., Analytica Chimica Acta, Vol. 351, No.1, pp. 151-158, 1997.

15. Kim, C.S., Lee, C.H., Fiering, J.O., Ufer, S., Scarantino, C.W., Nagle, H.T., IEEE Sensors Journal, Vol.4, No.5, pp. 568-575, October 2004.

16. Park, J., Kim, C.S., Kim, Y., Sensors and Actuators B, Chem., Vol.108, No.1-2, pp. 633-638, 2005.

17. Park, J., Kim, C.S., Choi, M., IEEE Transactions on Instrumentation and Measurement, Vol. 55, No. 4, pp. 1348-1355, August 2006.

18. Lide, D.R., CRC Handbook of Chemistry and Physics, Internet Version 2007, (87$^{th}$ Edition), <"http:/www.hbcpnetbase.com>, Taylor and Francis, Boca Raton, FL, 2007.

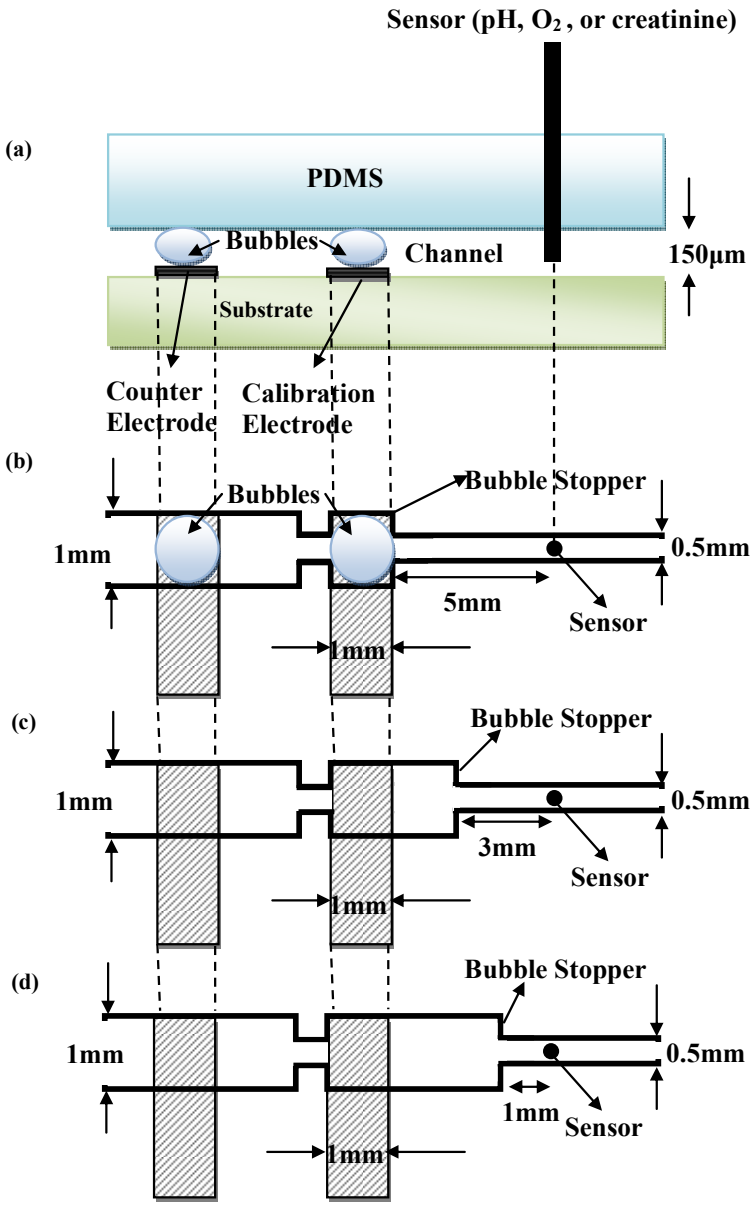


Figure 1. Side view and three different channel layouts. The bubble is generated and shifted towards bubble stopper.(a) Side view of fluidic chip. (b) Top view of the channel pattern for final distance of 5mm (i.e. no shifting). (c) final distance of 3mm. (d) final distance of 1mm.

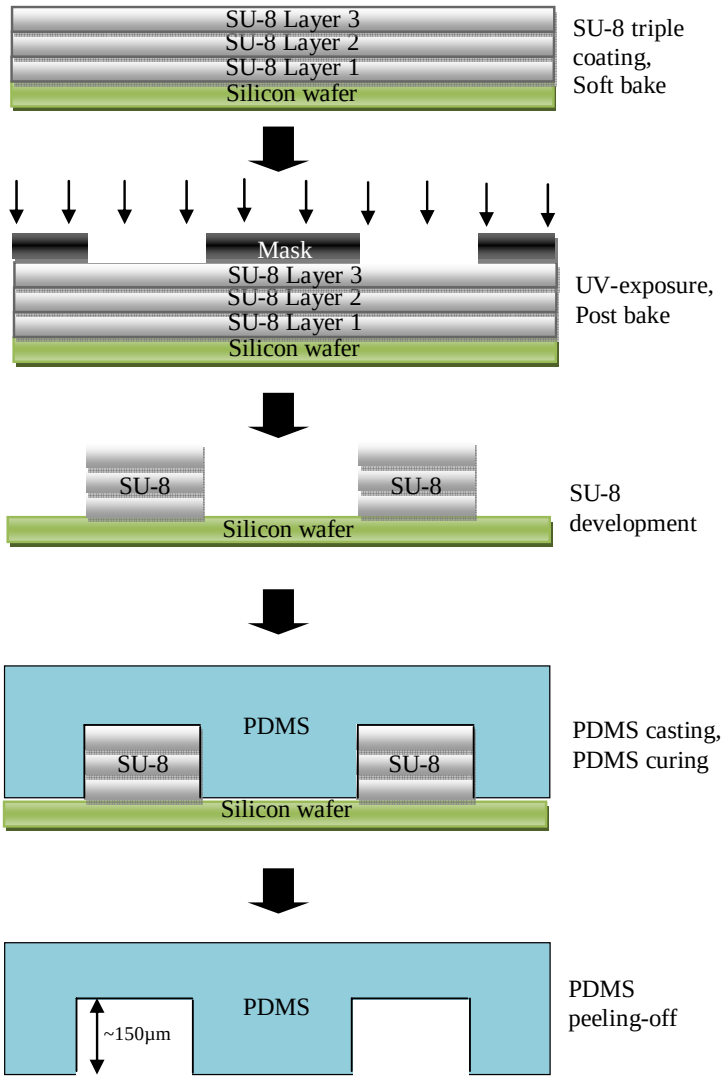


Figure 2. Microfabrication processes for PDMS cover layer.

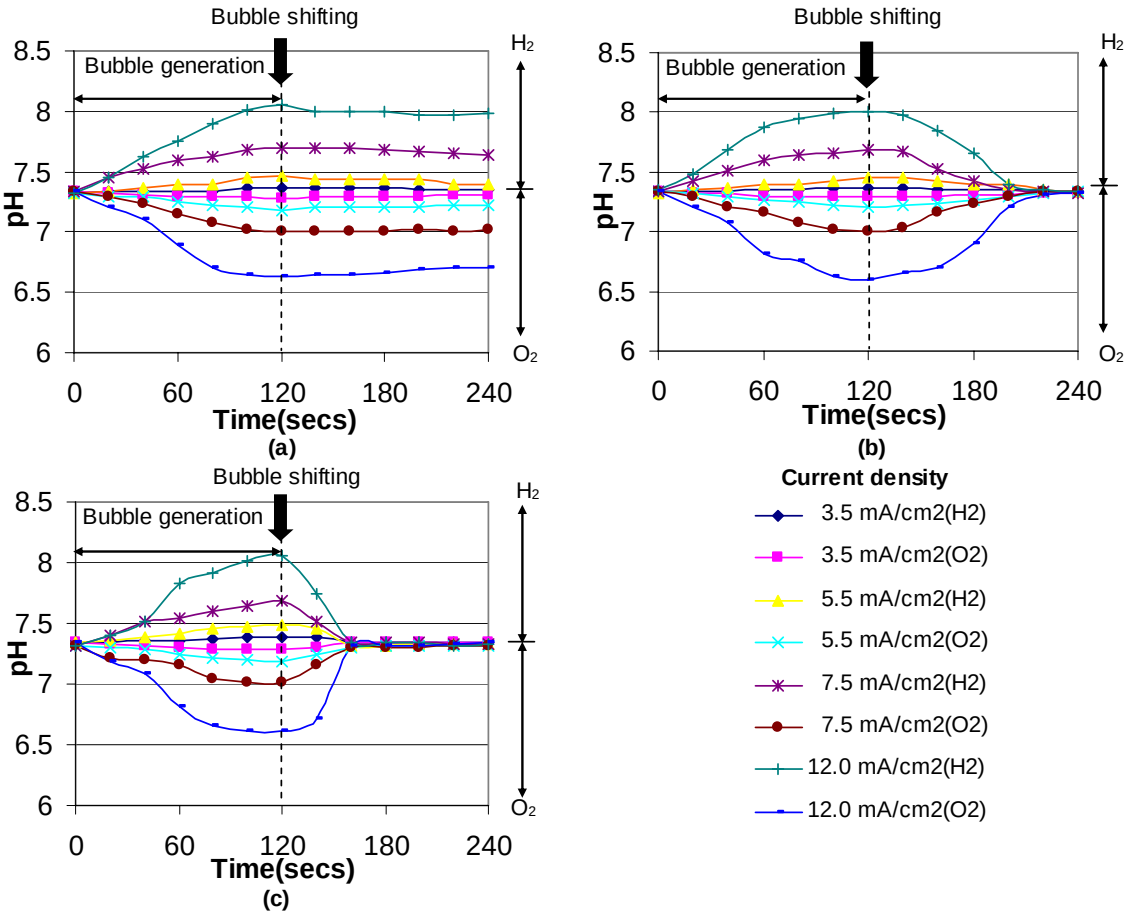


Figure 3. Responses of pH sensor for different distances between bubble and sensor, post bubble generation for 2 mins and shifting, at current densities of 3.5, 5.5, 7.5, 12.0mA/cm$^2$. (a) final distance of 5mm (i.e. no shifting). (b) final distance of 3mm. (c) final distance of 1mm.

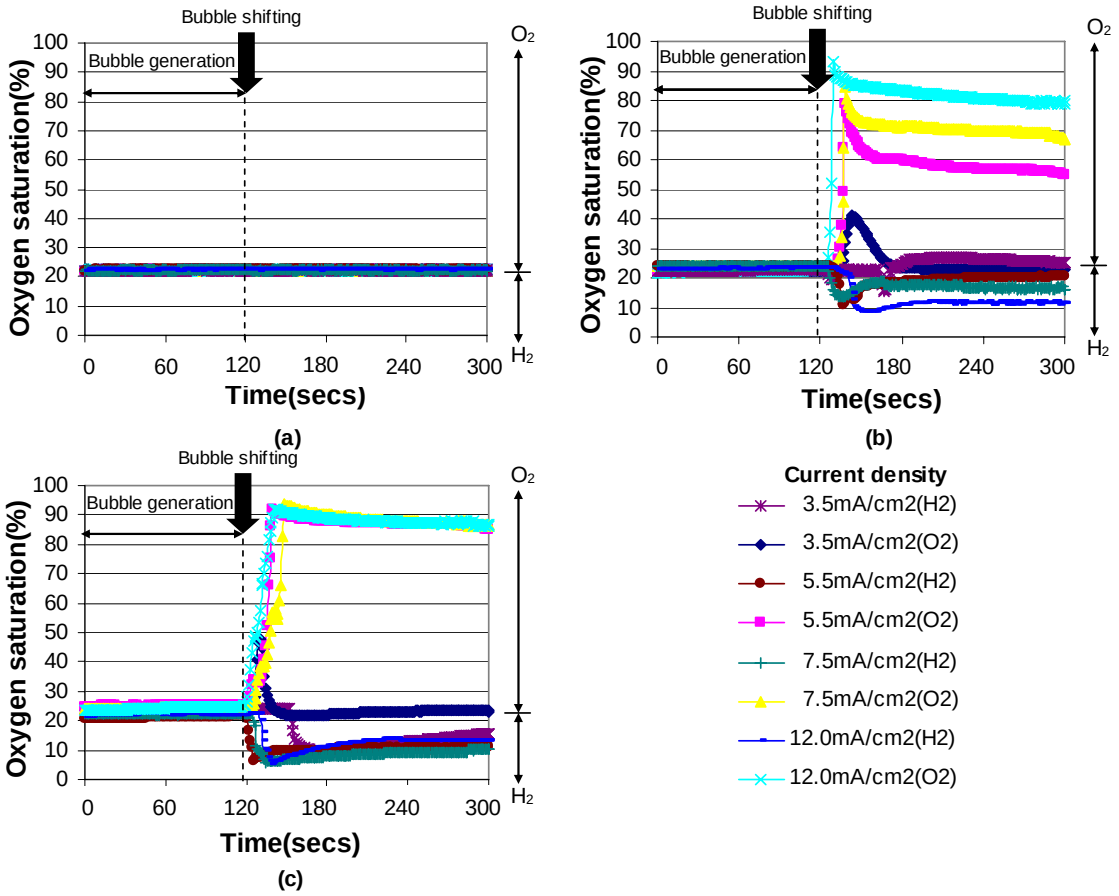


Figure 4. Responses of oxygen sensor for different distances between bubble and sensor, post bubble generation for 2 mins and shifting, at current densities of 3.5, 5.5, 7.5, 12.0mA/cm$^2$. (a) final distance of 5mm (i.e. no shifting). (b) final distance of 3mm. (c) Response for final distance of 1mm.

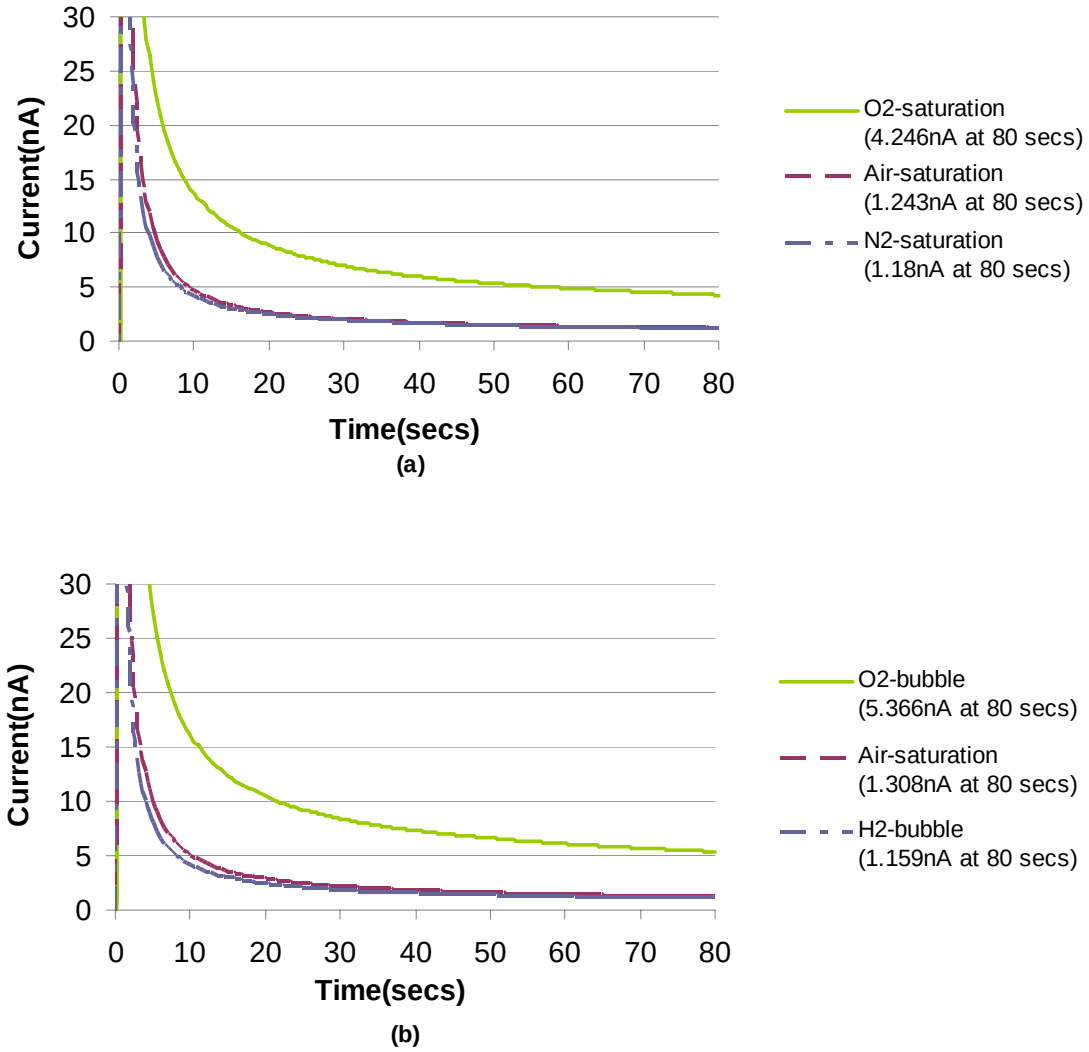


Figure 5. Chronoamperometric time responses for a creatinine concentration of 10mg/dl. (a) sensor placed in creatinine solutions saturated or depleted of oxygen by bubbling oxygen or nitrogen gases in a beaker. (b) sensor within the chip with creatinine solutions saturated or depleted of oxygen by bubbles in microfluidic channel at optimized final distance and current density.

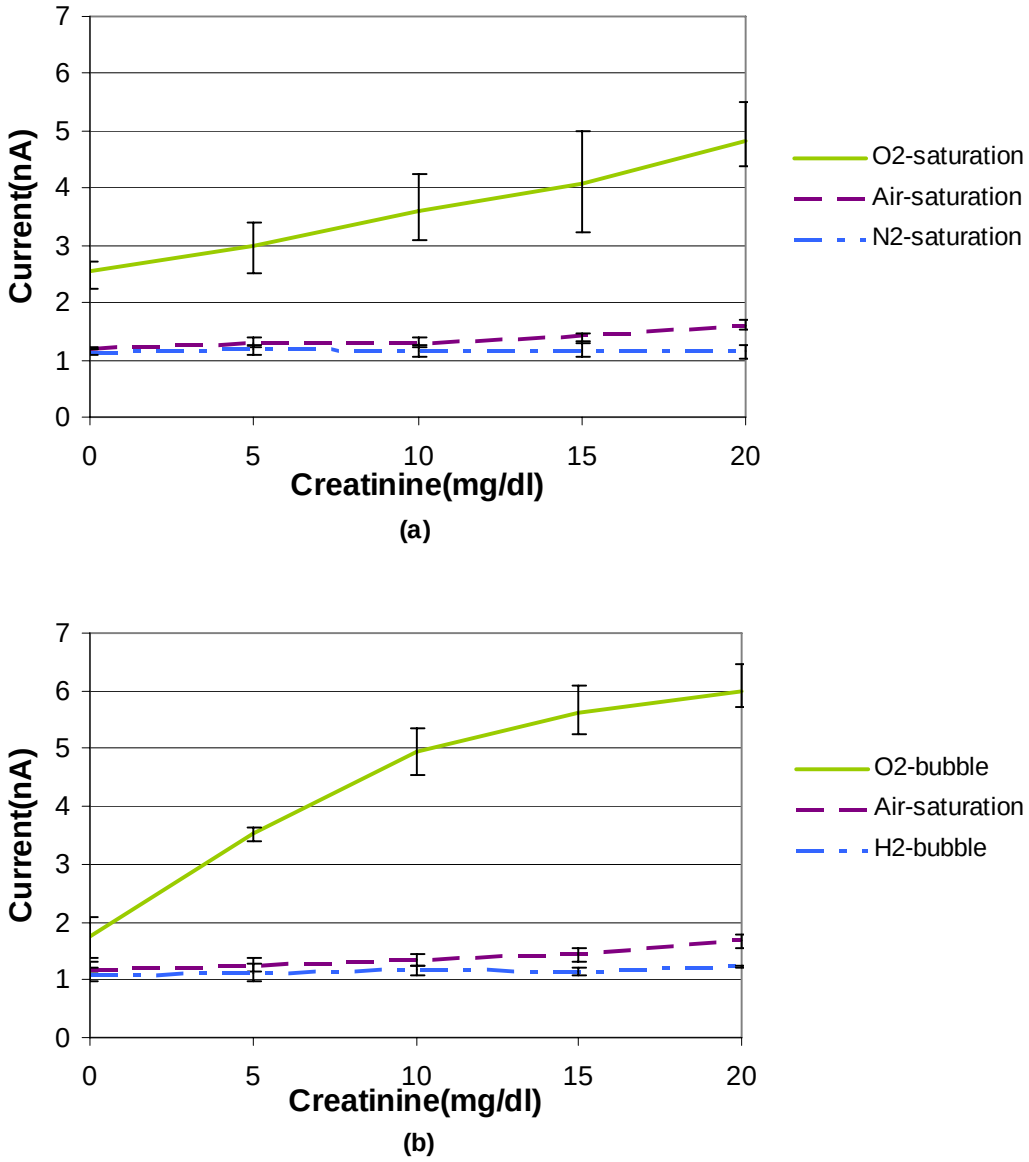


Figure 6. Creatinine concentration versus current (at 80 sec). (a) sensor placed in creatinine solutions saturated or depleted of oxygen by bubbling oxygen or nitrogen gases in a beaker. (b) sensor within the chip with creatinine solutions saturated or depleted of oxygen by bubbles in microfluidic channel at optimized final distance and current density.

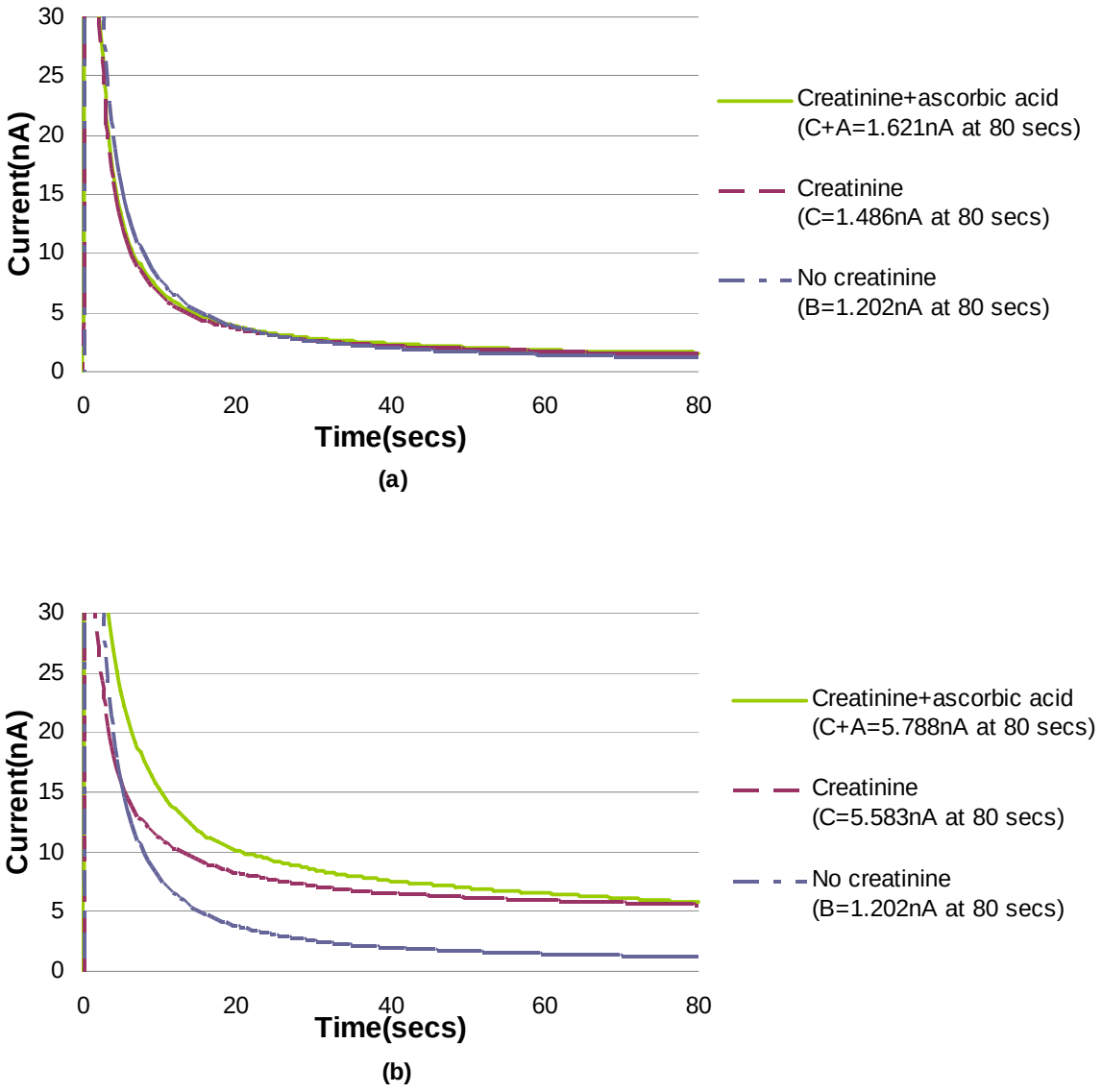


Figure 7. Chronoamperometric time responses of a same sensor for a creatinine concentration of 15mg/dl with and without 1mg/dl ascorbic acid. (a) responses in microchannel with creatinine solution saturated with air. (b) responses in microchannel with creatinine solution saturated with oxygen bubble.

# VITA

Nitin Radhakrishnan was born on January 14th, 1983 in Benghazi, Libya. In May 2005, he obtained his bachelor's degree in Electronics and Telecommunications from SCT College of Engineering, Trivandrum, India.

In January 2006, he enrolled at the University of Missouri-Rolla to pursue his master's degree in Electrical Engineering under the guidance of Dr. Chang-Soo Kim. During his time at UMR, he was employed as a Graduate Research Assistant at the Intelligent Microsystem Lab. He received his master's degree from UMR in December 2007.